Design of a two dipole magnet tagged photon spectrometer for the GlueX facility at the Jefferson Laboratory

G. Yang, J. D. Kellie.
Department of Physics and Astronomy, Glasgow University.

Abstract

A preliminary design of the GlueX two dipole magnet tagged photon spectrometer is shown in this paper. The spectrometer has a continuous straight focal plane which covers a wide momentum range of 25% to 95%E_0/c, where E_0 is the electron beam energy which will be designed to be 12 GeV. Optics calculations were carried out by using both TRANSPORT and TOSCA and the two results agree with each other. It was found by a finite element analysis that the pole gap of 30 mm will be reduced by the magnetic and the vacuum forces by around 0.2 mm when the magnets are operating at 1.5T. From a 3 dimensional magnetic field map obtained by TOSCA, it was found that the field non uniformity is of the level of 0.5%. To improve the field uniformity, very high quality steel is required along with precision machining and assembling. TOSCA simulation shows that there are only small variations in the tagger optics when the field uniformity becomes worse due to using construction quality steel and employing reasonable assembling techniques. A small change in tagger resolution has a negligible affect tagger on tagger performance; however, a small change in tagger dispersion alters the locations of the tagger focal plane detectors and also the tagger energy calibration. To investigate this effect, a field map is needed to determine the detector locations by ray tracing calculation.

1. Introduction.

The proposed GlueX project [1] requires tagged linearly polarized gamma rays to undertake the main goal of the GlueX project which is to search for specific aspects of quark interactions which will help to explain why quarks are confined. The required gamma rays will be generated by a coherent bremsstrahlung process [2] where the main electron beam interacts with a carefully oriented single diamond crystal radiator. A tagged photon spectrometer (hereafter we refer to it as tagger) is required to obtain the energy of each photon by measuring the energies of the energy degraded electrons. If the diamond radiator is thin enough, most of the electrons interact only once in the target via the coherent bremsstrahlung process. The photon energies are obtained by subtracting the energy of the energy degraded electron from the original electron beam energy. The main components of the tagger are its magnets, vacuum chamber and focal plane detector arrays. In this paper, a detailed design of the tagger apart of the detector arrays is presented.

2. Design considerations.

Conventional room temperature magnets will be used to build the tagger. Due to iron saturation effects, the magnetic field uniformity decreases with increasing magnetic field at relatively high fields. In order to obtain the required field uniformity and also keep the cost at a reasonable level, the operating field of the dipole magnets was set to be 1.5 T for a beam energy of 12 GeV.

Due to concerns about the mechanical stiffness, the availability of sufficiently large pieces of iron of the necessary quality and the availability of suitable manufacturers, a tagger consisting of two identical magnets in series was considered. By careful positioning of the two magnets it is possible to obtain a design that is equivalent to a single magnet configuration.

The bending angle of the tagger magnet was been set at 13.4 degrees. Although a larger bending angle improves the tagger momentum resolution, the resulting larger size of the magnet increases the cost considerably.

The tagger was specified to have a continuous straight focal plane, which should cover the energy range from 25%E_0 to 95%E_0, where E_0 is the original electron beam energy[1]. The photon resolution should be better than 0.5 %E_0 r.m.s along the focal plane and should be better than 0.1 %E_0 r.m.s in the photon energy range of 8~9 GeV. Considering the electron beam energy spread of 0.08% E_0 r.m.s., the electron energy resolution should be at least 0.06 %E_0 r.m.s.

3. The configuration of the Tagger.

The tagger plan view is shown in figure 1. It consists of two identical dipole magnets, a quadrupole magnet, and a vacuum chamber. The two dipoles are arranged in series. The separation between them is around 40 cm. The electron beam and the photon beam enter the first dipole magnet from the left side. The incident angle of the electron beam is 5.9 degrees. The two dipole magnets are not parallel. The angle between them is 0.892 degrees. These two dipoles are arrange in a way that, if we assume the field inside the magnet gap is constant and with a ideal sharp fringe field, the electron trajectory which goes through the right bottom corner of the first dipole will also goes through the left bottom corner of the second dipole. In this design, the energy corresponding to this special electron trajectory is 4.3 GeV. Therefore, the

energy degraded electrons with energy lower than 4.3 GeV will go through only the field of the first dipole and the electrons with energy larger then 4.3 GeV will see the fields of both dipoles. The vacuum chamber is narrow and relatively long. The vacuum chamber length along the exit window is around 11 meters. The width in the middle part is around 0.7 meter. The magnet pole shoes act as sidewalls of the vacuum chamber, and the vacuum chamber extends to the focal plane, where the detectors are located. In order to extend the vacuum out to the focal plane, without introducing any obstacles to the degraded electrons over the entire energy range, there is no sidewall along the exit edge of the vacuum chamber in the focal plane position. Instead, a very thin window is located there, which will seal the vacuum and allow the electrons through but not introduce too much multiple scattering. The vacuum force perpendicular to the flat surface of the vacuum chamber is around 70 tons. The vacuum chamber is not strong enough to support itself. To solve this problem, external ribs are used to support it. In the downstream zone (the right side, where the focal plane extends beyond the magnet), the external rib structure is wrapped all the way around the closed side of the vacuum box, while in the upstream zone, the vacuum forces are supported by rods attached to the magnets yokes as well as by external ribs. To guard against a buckling failure, the vacuum box is stiffened by means of cross ribs and edge flanges.

The dipole magnets are conventional C type magnets with rectangular pole faces. The yokes and pole shoes will be built using low carbon steel. A possible coil design could have coils wound from copper conductor having a 1.1 x 1.1 cm^2 square section with a central hole of 0.7 cm diameter for coolant flow. The conductor wires are wrapped with epoxy glass tape for electrical isolation. There are 90 turns on each coil, arranged in 6 layers of 15 turns. The parameters of a single magnet are shown in table 1.

Table 1 Magnet parameters

Parameters	properties
Total weight	~40 tons
Weight of bottom(or top) yoke	~13.5 tons
Weight of single pole shoe	~4 tons
Weight of a single coil	~0.4 tons
Height of the magnet	1.41 m
Width of the magnet	1.09 m
Length of the magnet	3.09 m
Gap height	3 cm
Magnetic field	1.5 T

A section view of the dipole magnet perpendicular to the magnet pole shoes is shown in figure 2. The top, bottom and return yokes are rectangular in shape. The pole shoe shape is also simple. There is a small step around the pole shoes, which provides a sealing surface between the pole shoes and the vacuum chamber.

A quadrupole is included in the design. Owing to the high energy of the incident electron beam, the length of the quadrupole is chosen to be 0.4m, and the distance between the quadrupole and the dipole should be not less than 0.5m as we need some space to accommodate the coils of the dipole and the quadrupole. The quadrupole parameters were chosen to minimize the contribution from the beam spot size on the

vertical beam height at the focal plane at around 9 GeV/c electron momentum, which is very important for a two-dimensional readout[2].

4. Optics calculated by TRANSPORT.

The optics of the tagger were calculated using TRANSPORT[3]. The main beam properties are listed in table 2. As input data for TRANSPORT, the scattered electrons are assumed to have the same size as the main beam but with a maximum beam divergence given by the formula for the angular divergence of bremsstrahlung electrons [4].

$$\Delta y' = \frac{4mc}{E_0} \times \frac{E_0 - E}{E}$$

where, E_0 and E are the original electron beam energy and the scattered electron energy respectively, m is the mass of electron, and c is the velocity of light in vacuum. Here, we assume the electron beam follows a Gaussian distribution. The object size is assumed to be equal to $2\Delta x$ (Δx is the square root of the variance of the beam radial distribution with about 68 % being located within the central $2\Delta x$ region.). The magnetic field used is 1.5 T. The field profile in the dipole is assumed to be constant within the central area with a ideal fringe field on both input and output edges. The electron resolution is defined as[5]

$$R = \frac{\Delta\omega}{D}$$

where $\Delta\omega$ is half the radial image size in the focal plane and D is the dispersion, both of which are calculated by TRANSPORT.

Some of the main factors of the optics calculated by TRANSPORT is shown in figure 3. It can be seen that the momentum resolution is well below 0.06% for the whole energy range, which satisfies the design requirement. The vertical image size, dispersion and beta (the angle between the beam trajectory and the focal plane) are the necessary data for designing the focal plane detectors. Due to the small main beam bend angle, the value of beta for the high electron energy part of the focal plane is around 6 degrees.

Table 2 Main beam properties

Parameters	properties
Transverse spot size at radiator Δx	1.7 mm r.m.s.
Vertical spot size at radiator Δy	0.5 mm r.m.s.
Tansverse beam divergence $\Delta x'$	0.020 mr r.m.s.
Vertical beam divergence $\Delta y'$	0.005 mr r.m.s.
r.m.s. energy spread $\Delta E/E_0$	0.080 % r.m.s.

5. Optics calculated by TOSCA.

In the TRANSPORT calculation, we used an ideal constant magnetic field with an ideal fringe field boundary. But for a real magnet, due to saturation effects, the magnetic field distributions are more complicated, especially at the magnet pole corners. In the present two-magnet system, we have to consider the electron trajectories through these corners or the areas near these corners. It is possible that the focal plane position and other properties will be affected by the magnetic field distribution. To study these effects, we need to know the magnetic field distribution.

By using TOSCA[6], 3 dimensional magnetic field distributions were calculated with a maximum magnetic field of 1.5T in the mid plane. It was found that the variation of the magnetic field over the central region (The central region is taken as the area lying inside the boundary defined by a line drawn round the pole edge two gap widths in from the pole stem [7].) is less than 0.5%. The effective field boundary (EFB) displacement with respect to the pole edge is around +2.5 cm around the pole edges; but near the pole corners, it is smaller by a few millimetres than at the middle part. The positive value of the displacement means the EFB is shifted outwards from the physical pole edge.

Figure 4 (a) shows the field variation along the main beam trajectory. It can be seen that, due to the small distance between the two magnets, the two magnets must be modelled together, rather than separately. Figure 4 (b) shows the field distributions along electron trajectories for electrons with energies from 3.9 to 5.0 GeV. It can be seen that even for an electron with an energy as low as 3.9 GeV, the electron trajectory goes through the fringing field of the second magnet. Also, electrons with energies in the range of 4.3 GeV to 4.7 GeV do not experience the full value of the field in the second magnet. This is significantly different from the magnetic fields used in the Transport calculation.

Based on the calculated magnetic field, the electron trajectories have been evaluated by using a group of carefully selected electron trajectories. The electron beam envelope and the focusing position can be determined, details of it will be shown elsewhere. The comparisons between the TRANSPORT and TOSCA results are also shown in table 3. Most of the focal plane positions are coincident with the TRANSPORT results. Only in the vicinity of 9 GeV are there some obvious differences. In the energy region from 3 to 5 GeV, which is affected by the more complicated corner magnetic field distribution and fringing field of the second magnet, no obvious changes have been found. The explanation may be that the small movement of the EFB due to the corner effect will reduce the bend angle. Whereas in contrast, the fringe field of the second magnet will increase it; so these two effects counteract each other.

Table 3 Comparison between the TRANSPORT and TOSCA results.

	Co-ordinates of focal plane position		Bend angle		Vertical height at focal plane		Horizontal spot size at focal plane	
	TR x(m), y (m)	TO x(m), y(m)	TR (degree)	TO (degree)	TR (cm)	TO (cm)	TR (cm)	TO (cm)
1 GeV	(0.869, 2.081)	(0.867, 2.077)	30.512	30.516	1.748	2.013	0.098	0.109
2 GeV	(1.112, 3.464)	(1.110, 3.458)	23.738	23.748	1.064	1.113	0.134	0.137
3 GeV	(1.311, 4.670)	(1.310, 4.667)	20.842	20.855	0.774	0.802	0.158	0.161
4 GeV	(1.491, 5.793)	(1.481, 5.757)	19.166	19.237	0.601	0.754	0.176	0.170
5 GeV	(1.770, 7.120)	(1.761, 7.094)	18.683	18.680	0.489	0.620	0.166	0.165
6 GeV	(2.061, 8.464)	(2.052, 8.439)	18.401	18.404	0.405	0.520	0.184	0.185
7 GeV	(2.328, 9.750)	(2.322, 9.731)	18.093	18.096	0.331	0.443	0.198	0.198
8 GeV	(2.580,10.99)	(2.597,11.06)	17.800	17.788	0.268	0.364	0.210	0.214
9 GeV	(2.819,12.21)	(3.295,13.75)	17.533	17.429	0.214	0.324	0.220	0.298

TR means TRANSPORT, TO means TOSCA.

6. Stress analysis for the dipole magnet.

When the tagger is operating at 1.5 T, the magnetic force between a pair of pole shoes is calculated to be around 150 tonnes. Additionally, because the pole shoes are acting as the lateral wall of the vacuum chamber, a significant vacuum force is applied to the magnet. Furthermore, weight of each magnet is around 40 tonnes. All these forces tend to deform the magnet structures slightly, causing a small reduction in the pole gap and a small distortion in the field distribution. Since these deformations may have important effects on the mechanical and optical properties of the tagger, a stress analysis was undertaken to calculate how the magnet body is deformed and subsequently estimate the effects.

For the stress analysis, ANSYS was used in conjunction with Autodesk Inventor Solid Geometry to simulate the behaviour of a mechanical body under structural loading conditions. A finite element mesh model was built based on the preliminary design of the tagger magnets. Only one magnet was modelled due to similar loads being applied to the two identical magnets. The mesh model contains 17854 nodes and 11033 elements. Because of the limited capability of the software, the whole magnet is modelled as one solid part. The material used for the yoke and pole shoes is low carbon steel AISI 1006. It was found that the maximum reduction in the pole gap is around 0.2 mm. Compared to the overall O-ring compression height of 6 mm, it is clear that this gap reduction will not affect the O-ring compression significantly. Since the magnet pole gap is 30 mm, magnet pole gap, the 0.2 mm gap reduction is only 0.7 % of the pole gap and hence the effect on the magnet field will be small. It was also found that the maximum deformation of the bottom yoke is only around 0.02mm. This is clear evidence that the magnet is sufficiently stiff, and is self supporting.

7. Effect of field non uniformity on tagger performance.

Ideally, we expect the magnet field to be constant and have an ideal fringe field. But in reality, the tagger magnet field uniformity is affected by many factors, such as the magnetic properties of the low carbon steel, the pole profile, the pole gap reduction due to the magnetic forces and any possible mechanical assembly errors. In this section we will discuss the effect of magnetic field non uniformity on the tagger optics.

Firstly, we consider how the steel properties affect the tagger. Three different types of low carbon steel have been investigated. One of them is the TOSCA default steel, which is believed to be a type 1006 steel annealed at a relatively high temperature [8]. The other two are AISI 1002 and AISI 1010.

Figure 5 shows the magnetic fields along a line perpendicular to the pole shoes in the mid plane. It can be seen that AISI 1002 gives the best field uniformity and AISI 1010 the worst performance. The optics are calculated by using the three different steels shown in figure 6. It can be seen that the tagger resolution, dispersion, vertical height and beta (the angle between the electron trajectory and the focal plane) are only slightly affected by the choice of steel. Small variations in the resolution, vertical height and beta will not affect the tagger performance. However, the variation in the dispersion will affect the detector energy calibration. Consequently, in order to measure electron energies accurately, the tagger should be carefully calibrated.

Secondly, the effect of the pole gap reduction caused by the magnetic forces on the tagger magnetic distribution was investigated. A comparison of the magnet field

with and without the pole gap reduction is sown in figure 7. It is found that a quadupole term appears in the filed for the magnet with a 0.2 mm gap reduction. Although the field becomes more non uniform, the optics calculated from this calculated field show that there are no significant changes in the resolution, dispersion and the vertical height.

Thirdly, we investigated how assembly errors could affect the tagger performance. Several TOSCA calculations have been carried out by taking into account possibly assembly errors. In these calculations, the second magnet was intentionally put into a wrong position, and various positioning errors investigated. They were

1. The second magnet is moved longitudinally +-2 mm along a straight line parallel to the long exit edge of the first magnet.

2. The second magnet is moved right or left 2 mm along a straight line perpendicular to the long exit edge of the first magnet.

3. The second magnet is rotated around the bottom right corner of the second magnet by an angle of +- 0.1 degree. The results show that these assembly errors do not have a significant effect on the tagger optics. The only obvious effect is that the energy calibration is changed slightly.

From the above results, it can be seen that magnetic field uniformities can be affected by many factors. This is because the magnet has a relatively high operating field and a relatively small the pole gap. The field uniformity could be improved, by using high quality low carbon steel, reducing the manufacturing and assembly errors and using a more sophisticated pole profile (such as a Rogowski pole profile). However, all these solutions will dramatically increase the overall cost. On the other hand, by choosing relatively poor quality (construction) steel and a simple pole profile, it is difficult to achieve the best overall field uniformity. Fortunately, the present tagger design is reasonably insensitive to field non uniformity. The tagger resolution, vertical image size, dispersion and the angle beta are only slightly affected by the field uniformity caused by construction quality steel and assembly errors. The small changes in resolution, vertical size and beta have no effect on the tagger performance. The only problem is that even a small change in the dispersion will affect the tagger energy calibration. However, if a detailed field map covering the whole tagger is available after the tagger is assembled, electron trajectories can be calculated by using this map and the energy range covered by each detector can be determined. Alternatively, the approach used to calibrate the Mainz tagger upgrade[9] can be followed by using the main electron beam to calibrate the tagger. This requires that the main electron beam energy is well known and can be tuned over a wide range.

8. Conclusions.

A wide momentum acceptance tagged photon spectrometer has been design for the Jefferson Lab GlueX project. This tagger has two identical dipole magnets and a continuous straight focal plane. Optics calculations have been carried out using both TRANSPORT and TOSCA and good agreement was obtained. Stress analysis shows that the pole gap reduction is around 0.2 mm when the magnets are operating at 1.5T. Simulations show that the tagger can tolerate the estimated field non uniformities. However, a full field map will be required for a sufficiently accurate focal plane detector energy calibration.

References

[1] http://www.halld.org/.
[2] R. T. Jones, Hall D Conceptual Design Report, v4.0 September 25 2002.
[3] TRANSPORT; A Computer Program for Designing Charged Partical Beam Systems. (CERN).
[4] J. D. Kellie, I. Anthony, S. J. Hall, I. J. D. Macgregor, A. Mcpherson et al. Nuclear Instrument and Methods in Physics Research A241 (1985)153-168
[5] Livingood, The Optics of Dipole Magnets, Academic Press New York and London, 1969.
[6] TOSCA; 3D Magnetic Field Computation (Vector Fields Ltd., 24 Bankside, Kidington, Oxford, UK).
[7] I. Anthony, J.D. Kellie, S.J. Hall and G.J. Miller, Nuclear Instrument and Methods in Physics Research A301 (1991)230-240.
[8] J. Karn and R. Wines, Finite Element Modeling of Permeability Differences in CEBAF Dipoles, J-Lab TN 99-016.
[9] C. Mcgeoge, private communications.

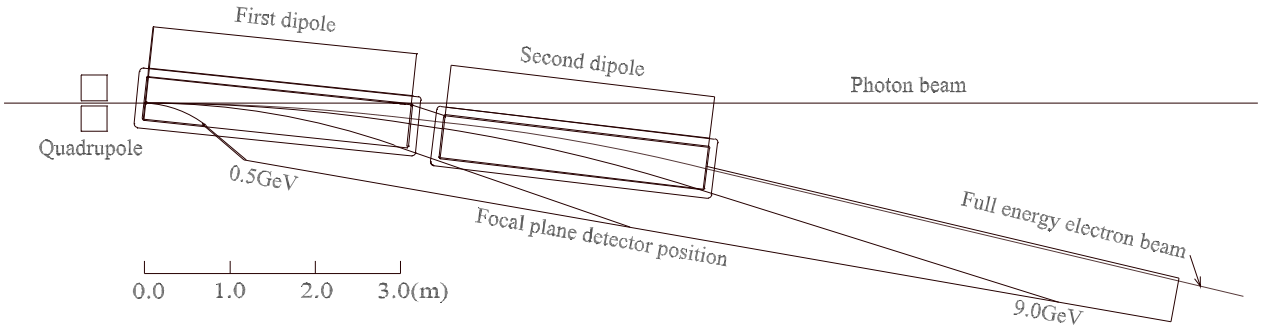

Figure 1. Plan of the GlueX 12 GeV tagged photon spectrometer.

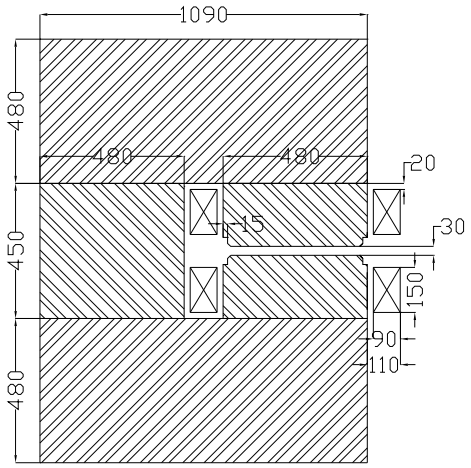

Figure 2. Vertical section through one of the two dipole magnets showing pole profile and coil geometry.

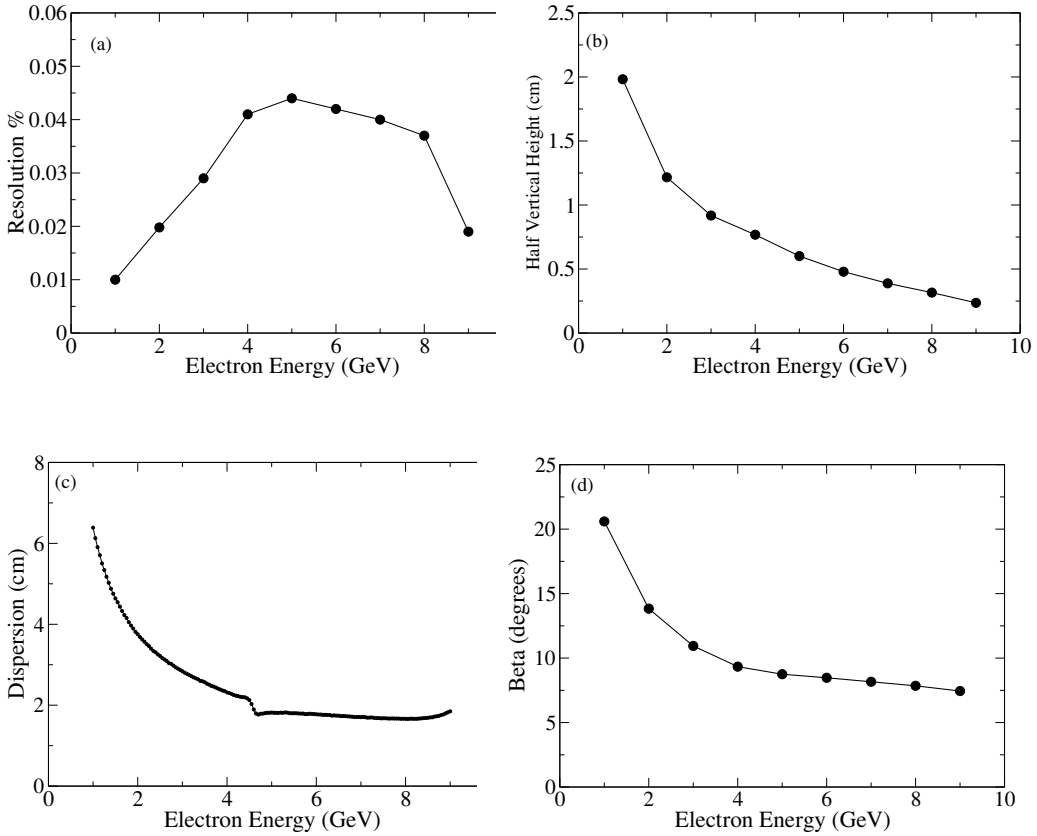

Figure 3. Spectrometer resolution, vertical image size, dispersion and angle beta calculated using TRANSPORT.

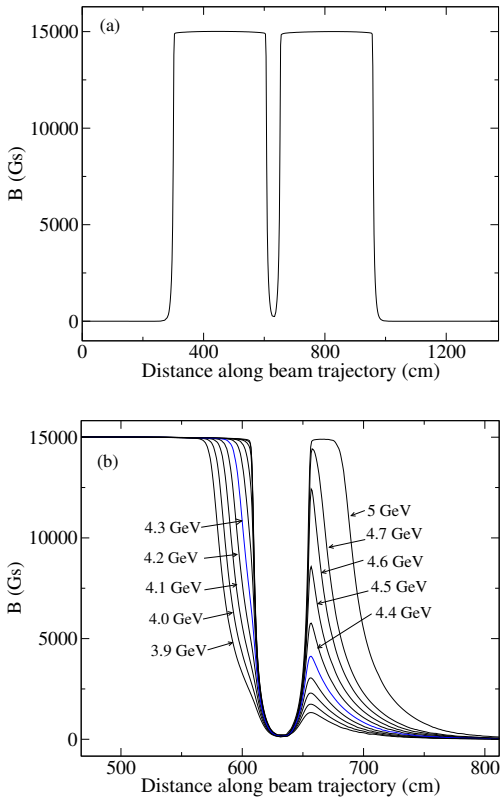

Figure 4. Calculated field variation at a maximum field of 1.5 T (a) along the 12 GeV main beam trajectory, and (b) along some selected beam trajectories with energies from 3.9 to 5.0 GeV.

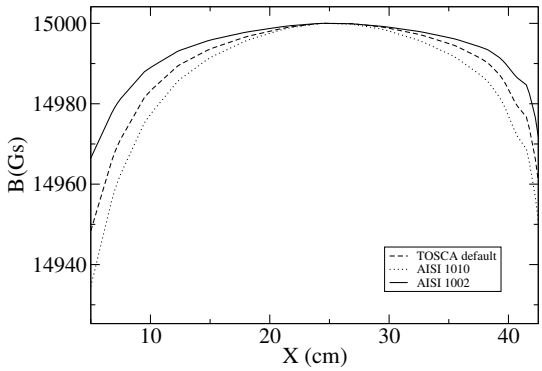

Figure 5. Calculated magnetic fields along a line perpendicular to the pole shoes for three different steels.

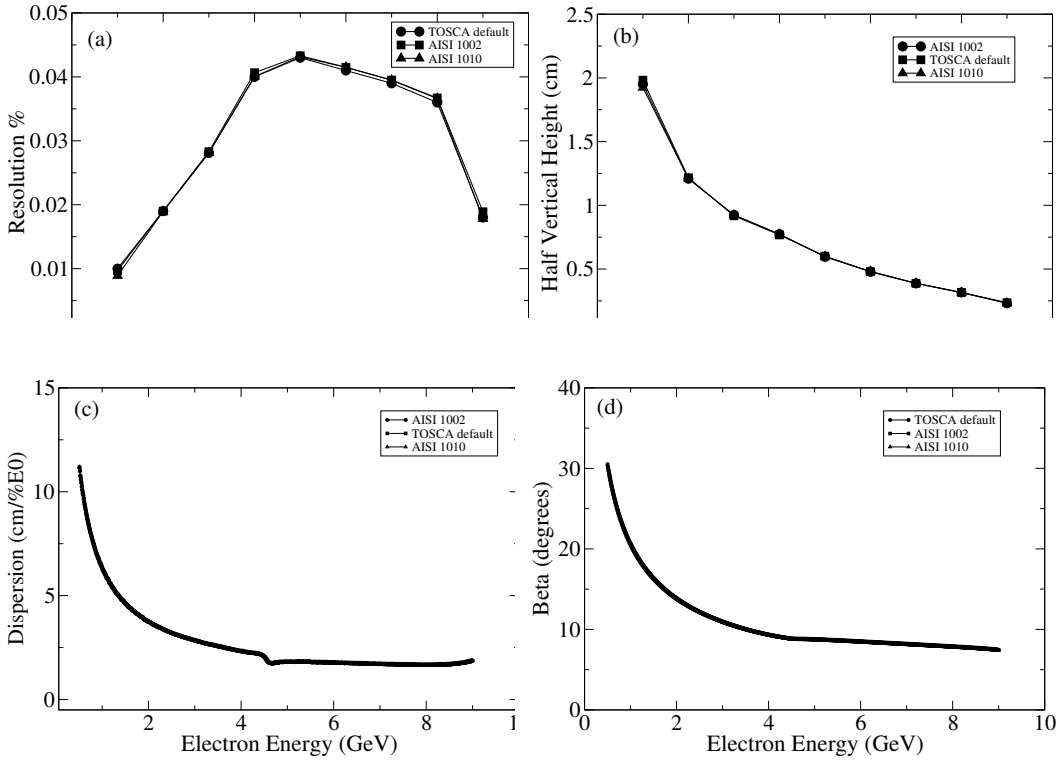

Figure 6. Spectrometer resolution, vertical image size, dispersion and angle beta calculated using TOSCA for three different steels.

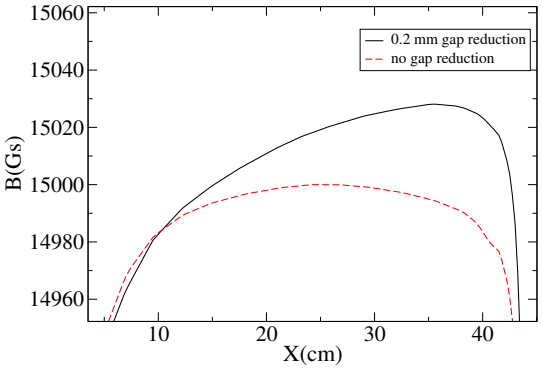

Figure 7. Calculated magnetic fields with and without the gap reduction along a line perpendicular to the pole shoes.